Sensory Neural Noise as a Limiting Factor in Visual Working Memory Precision in Neurotypicals and Schizophrenia

Woon Ju Park[1*], Megan Ichinose[2], Gengshi Hu[2], Geoffrey F. Woodman[2,3,4], Duje Tadin[5#], & Sohee Park[2,3#*]

[1]School of Psychology, Georgia Institute of Technology, Atlanta, GA, USA
[2]Department of Psychology, Vanderbilt University, Nashville, TN, USA
[3]Center for Integrative and Cognitive Neuroscience, Vanderbilt University, TN, USA
[4]Vanderbilt Vision Research Center, Vanderbilt University, Nashville, TN, USA
[5]Department of Brain and Cognitive Sciences, Department of Neuroscience, Department of Ophthalmology and Center for Visual Science, University of Rochester, Rochester, NY, USA

[#] Equally contributing senior authors

*Correspondence to:
Woon Ju Park
School of Psychology
Georgia Institute of Technology
654 Cherry St NW, Atlanta, GA 30332
E-mail: woonju@gatech.edu

or

Sohee Park
Department of Psychology
Vanderbilt University
111 21st Ave S., Nashville, TN 37240-7817
E-mail: sohee.park@vanderbilt.edu

ABSTRACT

The neural mechanisms that determine the capacity limits of working memory (WM) are not well understood, with traditional views identifying prefrontal circuitry as the source. Sensory encoding, however, remains an underexplored explanation for WM limits even though noise in sensory processing necessarily constrains brain functions that relay sensory inputs and mechanisms. Here we show that individual differences in internal sensory noise during visual processing predict visual WM capacity. Next, we show that the well-established WM deficits in schizophrenia can be linked to atypically high levels of visual sensory noise, providing a new explanatory framework for these deficits. Finally, we manipulated sensory noise levels in patients through transcranial direct current stimulation to the visual cortex, resulting in corresponding changes in visual WM precision. These findings show that sensory encoding fidelity may explain a significant amount of variance in WM function in both neurotypical adults and patients with schizophrenia.

MAIN TEXT

INTRODUCTION

Working memory (WM) is central to flexible and adaptive human cognition, enabling intelligent guidance of behavior [1]. The efficacy of WM is determined by its capacity, with capacity limitations leading to impaired information processing [2–4]. WM deficits are present in a wide range of neuropsychiatric conditions, including schizophrenia, anxiety disorders and dementias [5–9] and have a substantial impact on real-world functioning [10]. Thus, elucidating mechanisms that determine the capacity of WM is of broad scientific and clinical importance. WM storage involves coordinating functioning of multiple sensory, attentional, and cognitive control mechanisms [11–13]. Traditional theoretical approaches have focused on prefrontal access and control as the primary constraint on WM effectiveness [14–16], and it remains controversial whether sensory processing plays a key role in WM capacity limitations [17–19].

Limitations in sensory processing have been overlooked as a critical determinant of WM capacity largely because the fidelity of sensory processing far exceeds the WM capacity for sensory information [20]. At first glance, this makes sensory processing an unlikely culprit for WM limitations. This argument, however, fails to consider how variations in noise levels within sensory processing could cascade and affect brain functions that rely on sensory processing [21]. Noise is ubiquitous in neural processing [22]. It is present in sensory transduction, cellular processes of neurons, neural responses and motor outputs [23], limiting the efficiency of the brain's communication channels [24]. Noise present at earlier stages of sensory processing is subject to amplification during typical gain processes [21]. Thus, atypical increases in sensory noise may have unavoidable cascading effects on a wide range of brain functions that rely on sensory inputs, including WM.

Electrophysiological, neuroimaging, and brain stimulation studies demonstrate that sensory areas remain engaged during the maintenance of visual WM representations [25–27], forming the basis of the *sensory-recruitment hypothesis* [17,21]. Building on this view, we test the *sensory-noise hypothesis*, examining what specific factors of sensory processing determine the effectiveness of sensory recruitment, and in particular, how

sensory noise may limit WM capacity. We reasoned that visual WM may be particularly and uniquely vulnerable to sensory noise because it depends on the fidelity of sensory signals both for its initial encoding and for the maintenance of stored sensory information. In other words, if WM relies on the fidelity of sensory activity for both encoding and maintenance, then differences in sensory noise should translate into differences in WM capacity. In this framework, visual WM processing may be affected by sensory noise both in the feed-forward processing of visual information to be stored in WM and in the active maintenance of that information.

This framework makes several important predictions. First, it predicts that WM capacity limits will be systematically related to sensory noise levels in the general population. Second, it suggests that atypically high sensory noise could contribute to WM deficits observed in neuropsychiatric populations, such as schizophrenia, where limitations are often attributed to higher-level cognitive dysfunctions [28]. Third, the framework also predicts that these limits should be changeable if we could manipulate noise levels in the visual cortex itself.

We tested these predictions using converging methods of psychophysics and computational modeling (to estimate different sources of sensory noise), brain stimulation (to directly manipulate sensory noise), and clinical science. In our clinical work, we focused on schizophrenia where WM deficits have been proposed as an endophenotypic marker and a core feature of this condition [8,9]. WM deficits in schizophrenia have been characterized as a failure of high-level executive control [29]. However, schizophrenia is also associated with broadly atypical sensory processing [30–33], with implications for increased neural noise [34–36]. Together with our sensory noise hypothesis of WM, these suggest an as yet untested possibility that WM deficits in schizophrenia may derive from impaired sensory mechanisms.

RESULTS

To test whether sensory noise limits visual WM, we asked participants to complete both visual WM and orientation discrimination tasks, collecting data from 57 participants

(Study 1, 30 neurotypical adults (NT) and 27 individuals with schizophrenia or schizoaffective disorder (SZ), Table 1). The visual WM task required participants to remember locations and orientations of one, two, or four gratings and reproduce the orientation of a probed item after a 1 second delay with an input dial (Figure 1A; Methods). WM recall variance was the primary performance metric of interest. Less precise WM performance is reflected by higher recall variance, as demonstrated by the characteristic increase in recall variance (decline in precision of the reported orientation) as the number of items remembered increases [37,38]. Given that internal noise is hypothesized to add variability to, and/or destabilize, the internal representation [21,39], we hypothesized that elevated sensory noise would lead to higher WM recall variance.

Table 1. Demographic and Clinical Information for Studies 1 and 2.

	Study 1		**Study 2**
	SZ (n = 27)	**NT** (n = 30)	**SZ** (n = 20)
M/F	14/13	16/14	11/9
Age	45.04 (8.10)	44.96 (7.55)	48.60 (9.84)
Years of education	13.00 (1.80)	15.65 (2.61)	13.00 (2.08)
IQ[a]	102.30 (9.03)	106.14 (8.41)	102.25 (8.11)
Handedness[b]	+60.18 (13)	+72.59 (2.61)	+66.00 (53.87)
Ethnicity/Race:			
% Minority	62.96	36.67	70
BPRS	17.07 (6.61)	-	20.7 (10.95)
SAPS	18.37 (14.52)	-	28.25 (15.92)
SANS	28.81 (11.96)	-	29.85 (17.90)
CPZE	380.46 (460.90)		394.94 (271.43)

Mean values are shown with *SD* in parentheses. BPRS, Brief Psychiatric Rating Scale (Overall & Gorman, 1962); SANS, Scale for the Assessment of Negative Symptoms (Andreasen, 1983); SAPS, Scale for the Assessment of Positive Symptoms (Andreasen, 1984).
[a] National Adult Reading Test (NART; Nelson, 1982).
[b] Edinburgh Handedness Inventory (Oldfield, 1971).
[c] Chlorpromazine Equivalent Doses (mg/kg per day) (Woods, 2003).

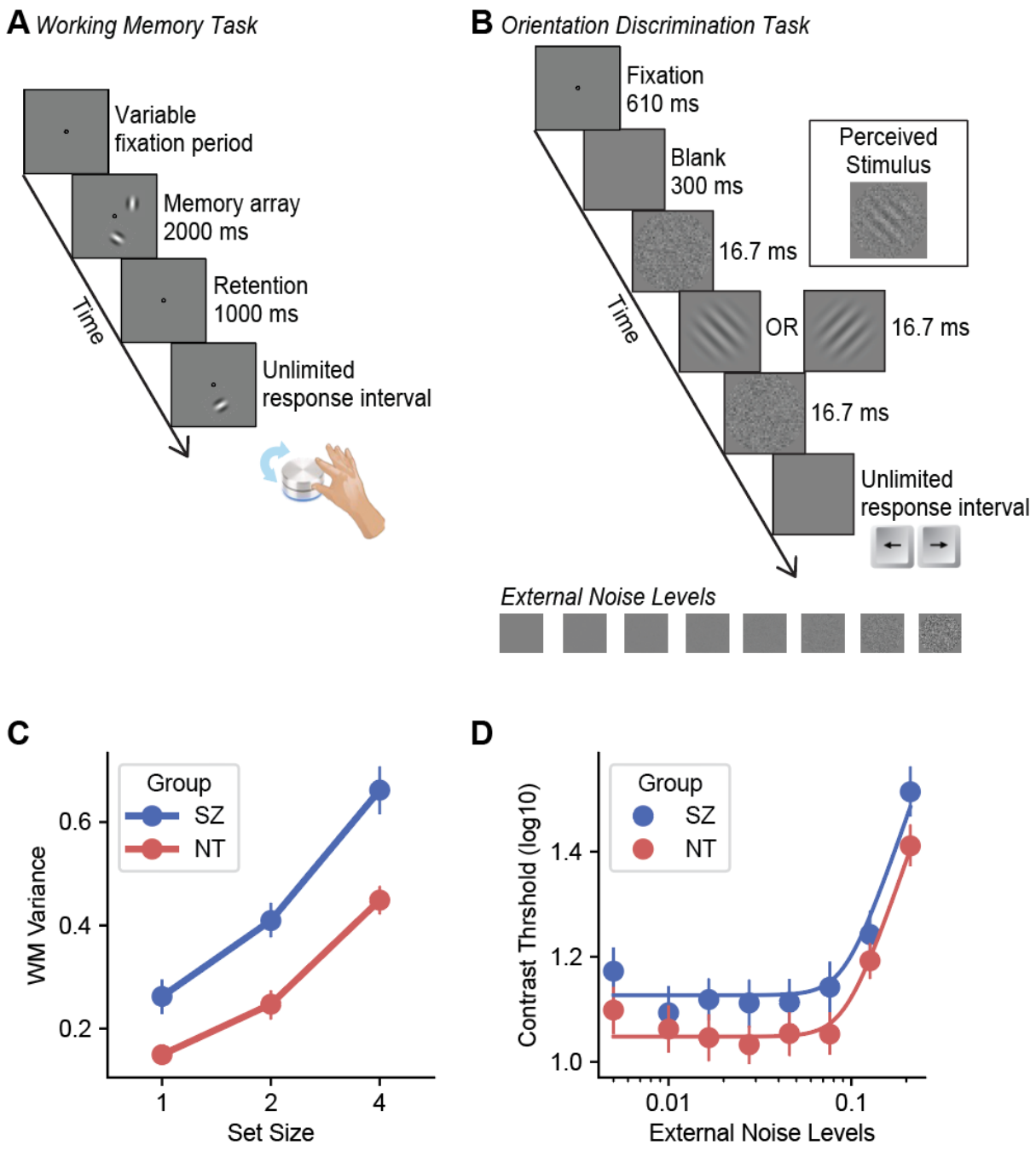

Figure 1. (**A, B**) Procedures for the visual WM task and the orientation discrimination task. See main text and Methods for details. (**C**) Results for the visual WM task. Both NT (red) and SZ (blue) showed worse WM performance with increasing set size, with SZ performing significantly worse than NT. (**D**) Results for the orientation discrimination task. Both NT (red) and SZ (blue) showed the characteristic non-linear increase in contrast thresholds with increasing external noise. SZ performed overall worse than NT, best explained by higher baseline internal noise and unfiltered external noise in SZ (relevant statistics are in the main text).

To quantitatively estimate noise in visual processing, we used the equivalent noise paradigm—a well-established psychophysical approach that has been extensively validated in both basic vision science [22,40,41] and clinical populations [42,43]. In this paradigm, participants discriminated coarse orientation differences (±45° tilt from vertical) of centrally presented gratings (1 cycle/°) embedded in varying levels of external noise (Figure 1B; Methods). Performance across these external noise levels was modeled with the Perceptual Template Model (PTM) [22]. A central strength of the equivalent noise approach is that it leverages a systematic manipulation of external noise to dissociate different sources of noise that limit perception. Specifically, the method provides quantitative estimates of (i) baseline internal noise, (ii) stimulus-dependent internal noise that scales with stimulus strength, and (iii) the ability of the visual system to filter out external noise in the stimulus (unfiltered external noise). The key insight behind the equivalent noise paradigm is that at low levels of external noise, performance is primarily limited by baseline internal noise, and external noise only begins to affect performance at high noise levels that exceed baseline internal noise.

By estimating sensory noise at both group and individual levels, we can (a) test for potential differences in sensory noise between SZ and NT, and (b) test whether these differences predict expected differences in WM. Importantly, we designed WM and noise estimation tasks to involve the same type of visual information, oriented visual stimuli, but to maximize differences in task demands and how subjects report their responses. The orientation discrimination task focused on stimulus visibility, estimated contrast thresholds in noise (i.e., stimuli shown at low signal-to-noise levels), and required only a coarse categorical response with a keystroke (±45° left vs right tilt). In contrast, the WM task used highly visible noise-free grating stimuli (i.e., high signal-to-noise) and required a precise report of the remembered orientation with a dial. If we had measured perceptual noise using one feature, like orientation, and memory using another feature, like color, then differences in perceptual discriminability between these features across individuals would be confounded with our measurements.

High baseline internal noise is associated with worse WM performance in NT

In the visual WM task, NT exhibited the expected pattern of greater WM variance with increasing set size (Figure 1C, red symbols; $F(2, 58) = 200.42$, $p < .001$, $\eta p^2 = .87$). In the orientation discrimination task, the same participants showed a highly characteristic nonlinear result, with contrast thresholds remaining fairly constant at low levels of external noise but increasing linearly (in log space) at higher levels of external noise (Figure 1D, red) [22]. These data were modeled with the PTM to estimate the baseline internal noise, stimulus-dependent internal noise, and the unfiltered external noise for each participant (see Methods).

To test our hypothesis that sensory noise predicts WM capacity in NT adults, we used a multiple linear regression with the noise estimates as predictors of the average WM recall variance. The model significantly accounted for 31.5% of the variance in WM precision ($F(3, 26) = 3.99$, $p = .02$, $R^2 = .32$, $R^2_{Adj} = .24$). However, only the baseline internal noise and unfiltered external noise were significant predictors of WM recall variance on their own (Figure 2A, red; baseline internal noise: $B = 1.02$, $SE = .44$, $t(29) = 2.31$, $p = .03$, $\eta p^2 = .17$; unfiltered external noise: $B = .21$, $SE = .09$, $t(29) = 2.31$, $p = .03$, $\eta p^2 = .17$). The stimulus-dependent internal noise ($B = -11.75$, $SE = 8.83$, $t(29) = -1.33$, $p = .20$, $\eta p^2 = .06$) did not significantly predict WM variance. This suggests that sensory noise associated with perceiving orientations is significantly linked to WM performance in NT adults.

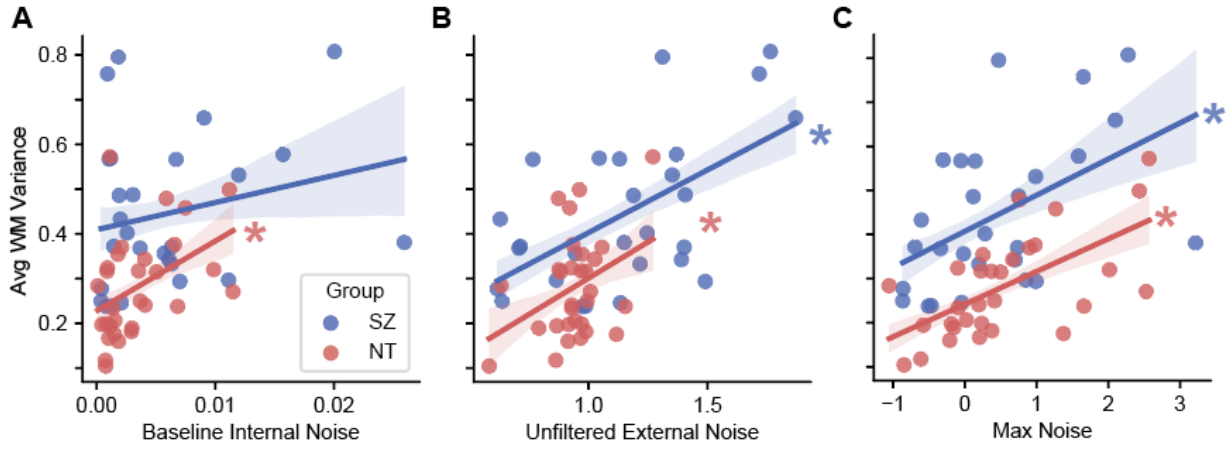

Figure 2. Sensory noise limiting orientation discrimination was associated with WM performance in both SZ (blue) and NT (red). (**A**) In NT, baseline internal noise and unfiltered external noise were significant predictors of WM performance. (**B**) In SZ, unfiltered external

noise was a significant predictor of WM deficit. (**C**) The 'larger' noise between the two (baseline internal noise vs. unfiltered external noise; z-scored per group) for each individual was significantly correlated with WM variance in both groups. This suggests that WM precision may be primarily constrained by the dominant source of sensory noise within an individual.

Elevated sensory noise is associated with impaired WM performance in SZ

If sensory noise is a key limiting factor of visual WM precision, then a deficit in WM may be due to a deficit in sensory processing. We tested this hypothesis in schizophrenia (SZ), a disorder with a well-established WM deficit [8]. In the WM task, individuals with SZ showed a marked impairment: the SZ group exhibited higher WM recall variance across all set sizes relative to NT (Figure 1C, blue; $F(1,55) = 18.04$, $p < .001$, $\eta p^2 = .25$). There was also a significant group by set size interaction ($F(2,110) = 5.05$, $p = .008$, $\eta p^2 = .08$) with patients showing greater deficits at larger set sizes. Because the WM task relies on reporting remembered orientation with fine motor movements, we also conducted a control motor precision task (where participants reproduced the orientation of visible gratings; see Methods) to test whether the observed group differences might be due to differences in motor precision. However, the results showed no significant differences between NT and SZ ($t(55) = 1.65$, $p = 0.11$, $\eta p^2 = .05$).

In contrast to the well-established WM deficit in SZ, much less is known about visual orientation processing in SZ, particularly limitations related to sensory noise. Our results from this task reveal a previously unknown perceptual deficit in SZ, with individuals with SZ exhibiting overall elevated contrast thresholds across a full range of external noise levels (Figure 1D, blue). These group differences were best explained by a model in which SZ and NT differed in the levels of both the baseline internal noise and unfiltered external noise. Specifically, the best-fitting model indicated a 61% increase in baseline internal noise along with a 21% increase in unfiltered external noise in the SZ group relative to the noise levels of the NT group ($R^2 = .98$). The model was significantly different from the null model where it was assumed that the two groups did not differ in their noise ($F(2, 26) = 29.95$, $p < .001$, $\eta p^2 = .70$, $\Delta R^2 = .03$), and was not significantly different from the full model where all three types of noise varied between the two

groups ($F(1,25) = .69$, $p = .41$, $\eta p^2 = .03$, $\Delta R^2 = .0004$). These findings together indicate that SZ is associated with elevated levels of sensory noise.

Critically, atypically elevated levels of visual noise in the SZ group predicted their WM performance. To examine this relationship in SZ, a multiple regression analysis was carried out with individually estimated baseline internal noise and unfiltered external noise, shown to be different in SZ, as predictors. The analysis revealed that the baseline internal noise and unfiltered external noise together accounted for 34% of the variance in WM recall performance ($F(2, 24) = 6.06$, $p = .007$, $R^2 = .34$, $R^2_{Adj} = .28$). However, only unfiltered external noise significantly predicted WM recall variance on its own in SZ (Figure 2B, blue, $B = .19$, $SE = .06$, $t(26) = 3.12$, $p = .005$, $\eta p^2 = .29$; baseline internal noise B = .29, SE = .44, $t(26) = .67$, $p = .51$, $\eta p^2 = .02$).

Our results are consistent with the hypothesis that the noise associated with sensory processing limits visual WM. In NT, baseline internal noise and unfiltered external noise predicted individual differences in WM performance. In SZ, both baseline internal noise and unfiltered external noise were significantly elevated, with variations in the latter predicting variability in WM. One possibility is that WM precision is primarily constrained by the ‘larger’ noise (baseline internal noise vs. unfiltered external noise) that overrides the other within an individual, similar to the rationale for the equivalent noise paradigm explained above. To explore this further, we computed z-scores for both baseline internal and unfiltered external noise separately for the NT and SZ groups. Then, for each subject, we kept only the larger of the two z-scores. This simple max operation is intended to capture noise that is more prominent for that subject relative to that subject's peer group (NT or SZ). We then correlated the result with WM performance and found that, for both NT and SZ, variability in sensory noise predicted visual WM precision (Figure 2C; NT: $r(28) = .62$, $p = .0002$; SZ: $r(25) = .49$, $p = .009$).

Direct manipulation of sensory noise impacts WM performance in SZ

Next, we tested the observed link between sensory noise and WM in a causal design using transcranial direct current stimulation (tDCS) to affect the noise in the sensory processing (Study 2). The goal was to causally manipulate sensory noise and measure its influence on WM performance in SZ. Using tDCS involves the application of low-

amplitude direct current to the scalp, thereby modulating the underlying excitability of cortical neurons in a polarity-specific manner. We focused on anodal stimulation because, in contrast to cathodal stimulation, it increases cortical excitability during and after stimulation, a modulation that is associated with increasing neural noise [44–46].

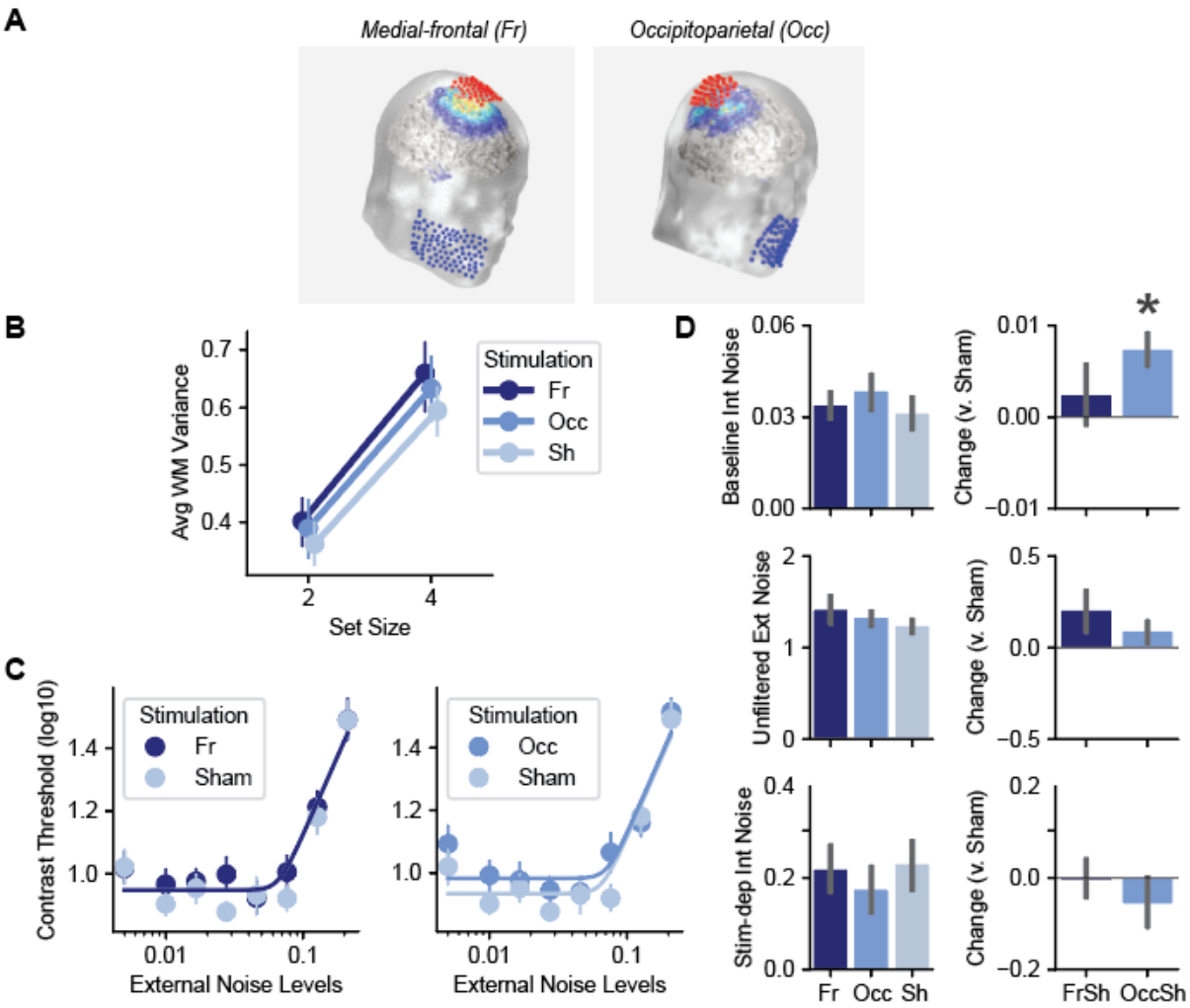

Figure 3. (**A**) Modeled current distribution for the medial-frontal and occipitoparietal stimulation sites. (**B**) Visual WM performance in SZ following tDCS across medial-frontal (Fr, darker blue), occipitoparietal (Occ, blue), and Sham conditions. (Sh, lighter blue), (**C**) Visual orientation discrimination performance following tDCS. (**D**) Changes in sensory noise estimated using PTM following tDCS. The parameter estimates from the hierarchical Bayesian model (Methods) are depicted for each stimulation conditions (left column) and for changes between active and sham conditions (right column; FrSh: medial-frontal vs. sham; OccSh: occipitoparietal vs. sham).

Twenty participants diagnosed with schizophrenia or schizoaffective disorder (SZ; Table 1) completed three stimulation conditions: anodal stimulation over occipitoparietal cortex, anodal stimulation over medial-frontal cortex, and sham (the location of which was randomly assigned to either occipitoparietal or medial-frontal cortex; Figure 3A). Stimulation over the occipitoparietal cortex served as our test condition based on prior work indicating that anodal stimulation over the visual cortex can heighten neuronal excitability underlying visual perception [47]. Active stimulation over the medial-frontal cortex served as a spatial active control condition due to its distance from the target sensory regions. Following 20 minutes of either active 2.0 mA stimulation or 20 minutes of sham stimulation, participants immediately completed the same WM task and orientation discrimination task described in the experiments above.

We first tested whether stimulation over the occipitoparietal cortex would increase sensory noise, as measured by PTM noise parameters derived from the orientation discrimination task. Participants' performance across the stimulation conditions again yielded the characteristic nonlinear dependency on external noise (Figure 3C). To characterize the effects of tDCS, the performances in the medial-frontal and occipitoparietal stimulation conditions were each compared with that in the sham condition separately using the PTM.

As hypothesized, visual orientation perception during the occipitoparietal stimulation was characterized by a significantly higher level of baseline internal noise compared to the sham condition (Figure 3D). Specifically, the effect of stimulation was best explained by a model in which active occipitoparietal and sham differed in the level of baseline internal noise. This model specified a 61% increase in internal noise with occipitoparietal stimulation relative to sham ($R^2 = .96$) and was significantly different from the null model in which all the noise parameters were equivalent with ($F(1, 27) = 4.36$, $p = .046$, $\eta p^2 = .14$, $\Delta R^2 = .01$), but not statistically different from the full model in which all noise sources differed from, the sham condition ($F(1, 27) = .42$, $p = .66$, $\eta p^2 = .02$, $\Delta R^2 = .001$).

The increase in sensory noise was only observed following the occipitoparietal stimulation. Compared to the sham condition, we found no evidence that medial-frontal

stimulation significantly impacted noise levels (Figure 3D). In particular, no model with any combination of varying noise parameters was significantly different from the null model (R^2 = .97) in which all the noise parameters were held constant across active medial frontal and sham conditions (all *F*s < 1.87, *p*s > .18).

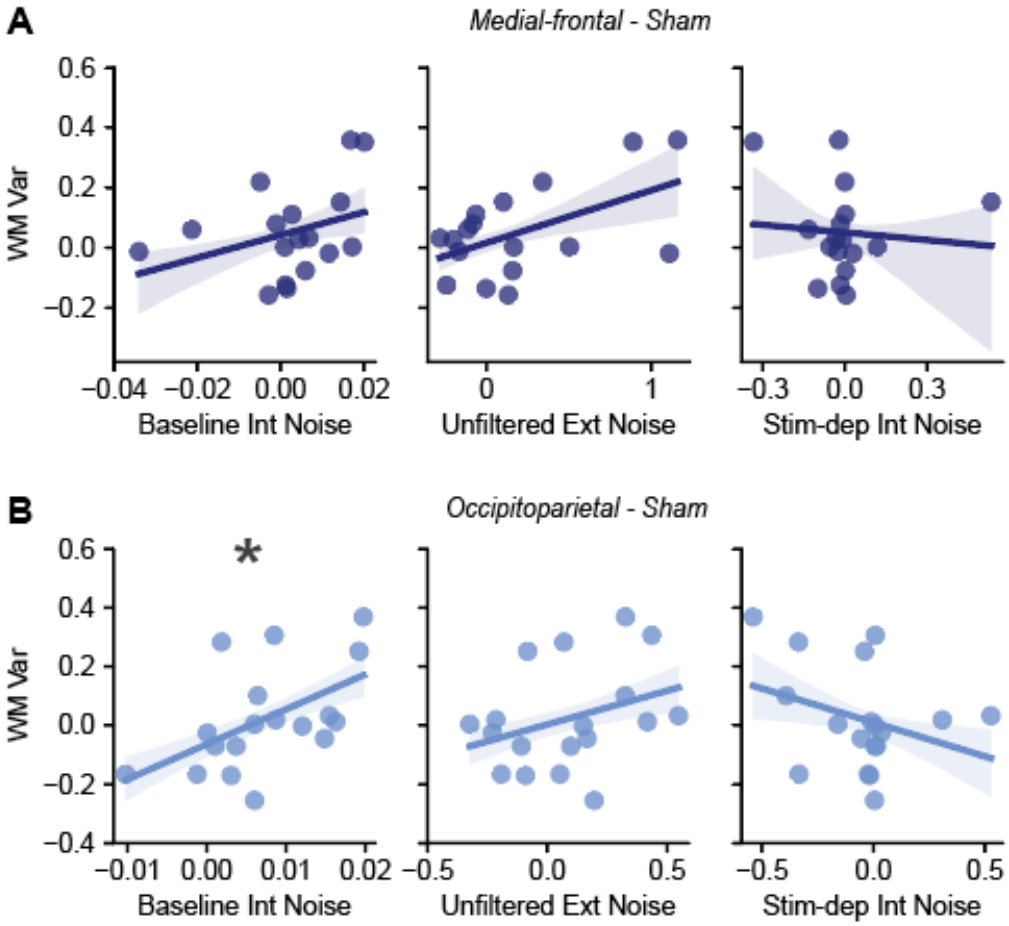

Figure 4. Relationship between changes in sensory noise and WM performance following tDCS stimulation in SZ. (**A**) Changes in sensory noise following the medial-frontals stimulation did not significantly predict changes in WM performance as compared to sham. (**B**) However, changes in baseline internal noise (left) following the occipitoparietal stimulation significantly predicted changes in WM performance.

The observation that anodal tDCS over the visual cortex increases sensory noise allowed us to test the hypothesized causal relationship between sensory processing and WM capacity. Namely, we examined whether tDCS-induced changes in baseline

internal noise in SZ would lead to concomitant *changes* in WM variance across individuals as compared to sham. On average, similar to Study 1, SZ showed worsening WM performance with increasing set size (Figure 3B, $F(1,19) = 61.52$, $p < .001$, $\eta p^2 = .76$), but, neither the medial-frontal nor the occipitoparietal tDCS stimulations influenced the overall WM recall variance (main effect of stimulation condition: $F(2,38) = 1.26$, $p = .29$, $\eta p^2 = .06$), with no significant interaction between set size and stimulation condition ($F(2,38) = .17$, $p = .84$, $\eta p^2 = .009$).

However, the *concurrent changes* in sensory noise and WM performance within individuals were significantly correlated with each other following only the occipitoparietal stimulation as compared to sham (Figure 4B). In other words, although stimulation did not alter WM performance at the group level, individuals who showed a greater stimulation-related increase in baseline internal noise compared to sham exhibited greater impairment in WM performance, but only following occipital stimulation. A multiple linear regression model with changes in all noise parameters (stimulation – sham) as predictors explained changes in WM performance (stimulation – sham), accounting for 45% of variance ($F(3,14) = 3.79$, $p = .04$, $R^2 = .45$, $R^2_{Adj} = .33$), and only the changes in baseline internal noise on its own significantly predicted the changes in WM variance in these respective conditions (Figure 4B, left; $B = 12.56$, SE = 5.31, $t(17) = 2.36$, $p = .03$, $\eta p^2 = .29$; stimulus-dependent noise: B = -.30, SE = .15, $t(17) = -2.05$, $p = .06$, $\eta p^2 = .23$; unfiltered external noise: $B = .05$, SE = .16, $t(27) = .29$, $p = .78$, $\eta p^2 = .006$). In contrast, changes in the noise parameters following medial-frontal stimulation as compared to sham did not significantly explain changes in WM variance (Figure 4A; $F(3,13) = 1.72$, $p = .21$, $R^2 = .28$, $R^2_{Adj} = .12$). In other words, increases in baseline internal noise specifically after occipitoparietal stimulation predicted the degree to which WM became less precise and more variable.

DISCUSSION

Our study provides a set of observations supporting the central role of sensory noise in determining WM limits. The findings suggest that noise present in early stages of visual processing limits how accurate WM representations can be, affecting their precision at

recall. Using a computational model of perceptual processing [22,48], we show that individual differences in sensory noise can both explain individual variability in WM capacity and account for the well-established WM deficit in individuals with schizophrenia. Our manipulations of sensory noise with tDCS over the visual cortex provided a causal link between sensory processing and WM, where changes in internal noise with stimulation resulted in corresponding changes in the precision of WM recall. These findings indicate that lower-level sensory mechanisms contribute to capacity limitations typically attributed to high-level cognitive processes. We conjecture that visual WM is particularly vulnerable to sensory noise not only because it relies on sensory information as its input, but more importantly because it recruits sensory mechanisms for the maintenance of stored information [17,21]. One putative advantage of involving sensory mechanisms for information maintenance in WM is the high fidelity of sensory processing. We posit that this is also what makes the precision of visual WM particularly sensitive to noise levels within the visual process.

Because effective WM performance depends on multiple stages, including encoding and maintenance [49,50], it is also susceptible to processing inefficiencies, including noise, at each of those stages [4]. Both the sensory recruitment hypothesis and the sensory noise hypothesis suggest that sensory areas are actively recruited in these stages, where the fidelity of sensory representations directly influences WM precision. While our study does not directly distinguish the effects of sensory noise during encoding vs. maintenance stages as we did not isolate delay-period activity, it is plausible that sensory noise also influences maintenance, particularly more so given that neural activity for memory retention in the sensory cortex is generally weaker than when a physical stimulus is present [51], allowing more room for noise to exert its effect.

Our support for the idea that sensory noise affects WM storage does not preclude a role of the prefrontal circuitry in determining WM capacity [18]. Instead, our findings add a complementary view from the sensory processing perspective: in tasks that rely on sensory details, such as orientation, color, or location, the fidelity of sensory cortex representations is crucial. The persistence of WM capacity limits even when visual stimuli remain in view suggests that WM is not simply about maintaining perceived input

in memory [52], but about performing simultaneous operations on multiple representations. In this context, sensory noise is critical as it constrains the precision with which representations can be manipulated and compared. At the same time, cognitive processes such as attentional lapses also shape how effectively these noisy sensory representations are used [53]. In this perspective, WM capacity is a joint outcome of limitations in representational fidelity and the efficiency of higher-order control processes.

Our results also show that the WM deficits in SZ, traditionally associated with impairment in prefrontal processing, can be explained by elevated levels of sensory noise within an individual. This is consistent with a recent finding that implied faster WM decay in SZ [54], which could result from noisy sensory representations. At the group level, SZ participants' WM precision was best explained by their ability to filter out external noise. In the PTM, external noise filtering occurs at the earliest stages of visual processing, where ‘templates’ selectively enhance relevant signals and suppress irrelevant external noise. The effectiveness of this filtering depends on the tuning properties of these templates. Notably, prior work has demonstrated broader orientation tuning in SZ [55], which could explain elevated levels of unfiltered external noise observed in our study. It is possible that noisy representations due to broader orientation tuning in SZ are having a larger effect on WM capacity than elevated baseline internal noise.

Importantly, we show that direct manipulation of baseline internal noise through brain stimulation affects WM capacity in SZ. Anodal tDCS is known to increase cortical excitability [56,57], which can modulate the spontaneous fluctuation in neural activity. Given the lack of temporal precision and task-specificity, it is less likely that the stimulation selectively enhances task-related activity (stimulation is continuously applied for 20 minutes prior to completing the tasks). If the tDCS rather amplifies random neural variability, it can reduce the overall signal-to-noise ratio in neural responses by increasing baseline neural noise. Our findings are not at odds with the previous observation of increased visual sensitivity to low-contrast stimuli following anodal tDCS [58], as in our task, increased excitability would amplify the responses for not only the target signal (oriented grating) but also the external noise added to the stimuli. It is also

worth noting that the effects we observed were individual-specific: patients who showed an increase in baseline internal noise following tDCS to the occipitoparietal cortex also exhibited a corresponding decline in WM precision. This pattern may suggest a considerable heterogeneity in SZ, where not all patients respond to interventions in the same way. Recognizing this variability provides critical considerations for designing individualized intervention strategies.

Our findings identify early visual processing as a significant WM bottleneck in SZ. Elevated sensory noise in the system has far-reaching consequences in addition to contributing to WM deficits. Other aspects of visual information processing may also be impacted by increased sensory noise in SZ, including motion perception [35] and visual context processing [59]. Furthermore, face discrimination deficits associated with increased internal noise in SZ [36] could potentially cascade to social cognition impairments. Increased sensory noise has also been observed in individuals with autism spectrum disorders (ASD) [43,60], a population similarly noted for their WM deficits [61,62]. In both SZ and ASD, elevated neural noise may reflect or even contribute to an excitation/inhibition imbalance in cortical circuits [34], a mechanism that has been widely proposed in both populations [63–65]. This suggests that neural noise may not merely be a byproduct of atypical sensory processing but may play a mechanistic role in shaping higher-level cognitive outcomes such as WM. Understanding how sensory noise interacts with developmental and neuroanatomical factors, as well as its potential interactions with neuropsychiatric medications for each condition, could provide key insights into the shared and distinct pathways through which WM deficits emerge in a wide range of neuropsychiatric disorders [6,49,66–69].

In conclusion, we report both the correlational and causal evidence for the effects of sensory noise on WM capacity. We conclude that the noise that limits the efficiency in perceptual processing plays a critical role in constraining WM recall precision. The results offer new insights into the sensory recruitment hypothesis of WM and highlight sensory noise as a possible target for intervention (e.g., through brain stimulation or perceptual training) that could enhance WM capacity in populations whose WM deficits have been primarily associated with cognitive dysfunctions.

METHODS

PARTICIPANTS

Demographic and clinical information for participants who completed Studies 1 and 2 is summarized in Table 1. Twenty-seven (48% women; Study 1) and 20 (45% women; Study 2) medicated and clinically stable outpatients with chronic schizophrenia or schizoaffective disorder (SZ) were recruited from outpatient facilities in Nashville for participation. Diagnoses were made or confirmed according to the Diagnostic and Statistical Manual of Mental Disorders, Fourth Edition, Text Revision (DSM-IV-TR) criteria using the Structured Clinical Interview for DSM-IV (SCID-I/P) [70]. SCIDs were administered by masters-level clinical psychology graduate students.

In Study 1, 30 (47% women) neurotypical controls (NT) were recruited from the same metropolitan area through advertisements. NT had no history of DSM-IV Axis I disorders or family history of psychosis. We estimated premorbid IQ using the North American Adult Reading Test (NART) [71]. SZ and NT in Study 1 were matched on age, estimated IQ, and handedness but not on years of education ($t(55) = 4.18$, $p < .01$). Exclusion criteria included a history of head injury, neurological disorder, or substance abuse in the 6 months preceding the study.

All SZ participants were taking medications at the time of the study; in Study 1, 26 were taking atypical antipsychotics, 1 was taking a typical antipsychotic, 4 were taking mood stabilizers, and 10 were taking SSRIs, and in Study 2, 19 were taking atypical antipsychotics, 1 was taking a typical antipsychotic, 1 was taking a mood stabilizer, and 10 were taking SSRIs. Antipsychotic doses were converted to chlorpromazine equivalents for comparative analyses. Symptom severity in SZ was assessed with the Brief Psychiatric Rating Scale (BPRS; Overall and Gorman, 1962), the Scale for the Assessment of Negative Symptoms (SANS) [72], and the Scale for the Assessment of Positive Symptoms (SAPS) [73]. All participants were screened for normal or corrected-to-normal vision with the Snellen test of visual acuity. For the Snellen test, participants read through the chart using one eye at a time, viewed the letters from a distance of 20

feet, and read letters from the top of the chart aloud to an experimenter who scored their performance. Based on this viewing distance and the reference standard (20/20), the 8th row of letters from the top of the chart consisted of letters subtending an angle of 5° with each letter part subtending 1°.

All participants provided written informed consent to study procedures approved by the Vanderbilt University Institutional Review Board and were compensated for their participation at a rate of $20 per hour.

STIMULI, TASKS, AND PROCEDURE

All tasks and stimuli in Studies 1 and 2 were programmed in MATLAB and Psychtoolbox [74,75] and presented on a linearized monitor (20-inch Sony CRT; 1024 x 640 resolution; 120 Hz) on a gray background. A chin rest was used to maintain viewing distance at 77 cm with each pixel subtending 0.036°. An experimenter was present in the room during both visual discrimination and working memory tasks to encourage task engagement. Task order was counterbalanced across participants.

Visual Working Memory Precision Task

To assess visual WM, participants completed a WM task in which they were instructed to remember locations and orientations of sinewave gratings (1 cycle/deg) in a two-dimensional raised cosine envelope (radius = 1°). All gratings were presented at maximum contrast to ensure visibility. The trial procedure was as follows: first, a memory array consisting of one, two, or four oriented gratings was presented for 2 s. Orientations were randomly selected from all possible options [-90°, 90°] with the constraint that orientations within a given memory array were unique. Grating locations for each trial were randomly chosen from eight positions around an invisible circle (radius 4°) centered on a fixation point. After a short delay (1 s), a new, randomly oriented [-90°, 90°] grating appeared at one of the prior locations (test probe). Participants used an input dial (PowerMate USB Mulitmedia Controller; Griffin Technology) to adjust the test probe's orientation so that it matched the orientation of the grating presented at that same location. Participants were asked to be as precise as

possible when matching orientations and responses were untimed. Participants indicated their final response by pressing down on the dial, leading to a 3 s inter-trial interval. Trials began with a centrally-presented dynamic fixation sequence [76]. Participants completed a total of 450 trials, split equally into 10 blocks with rest periods lasting a minimum of 30 s.

Because group differences in ability to use the manual dial may confound hypothesized group differences in WM precision, participants also completed a short motor precision task that did not tax memory. Participants completed the motor precision task prior to the WM task in order to become acclimated to using the manual dial. Trials involved presentation of a randomly oriented grating located at one of eight positions around an invisible circle (radius 4°) that remained on the display. A randomly oriented grating was then presented at the center of the display, and participants were instructed to use the manual dial to adjust the orientation of this central grating until it was aligned with the orientation of the first grating, which remained on the display until the participant's response was submitted. Consistent with instructions on the WM task, participants were asked to be as precise as possible when matching orientations and responses were untimed. Participants completed a total of 24 trials such that each of the 8 possible grating locations was sampled three times.

This manual recall method has been used with both healthy adults and psychiatric populations to obtain a more detailed, continuous measure of visual WM precision compared to typical binary match/non-match response paradigms [21,77]. Importantly, this method enables WM performance to be analyzed as a distribution of recall errors (the difference between input response and target orientation) with accompanying descriptive properties of the distribution. As the number of visual features or items to be remembered increases, the decline in recall precision is captured by the increasing variance of the error distribution.

Orientation Discrimination Task

Participants performed a coarse orientation discrimination task [43] where they judged the tilt of centrally presented gratings with the same spatial frequency and size as those in the WM task (tilted ±45° from vertical). Gratings were temporally embedded in two

independent external noise samples. The grey-level pixel values for external noise were sampled from a Gaussian distribution with a mean of 0 and SD that varied across trials, such that its root mean square contrast defined the external noise level to be one of 8 set levels ranging from 0-21% (0, 0.3, 0.61, 1.24, 2.51, 5.1, 10.3, or 21%). The rapid temporal succession of noise, stimulus, and noise frames (16.7 ms duration per frame) results in an intentional perceptual merging of the grating and noise frames that is consistent with PTM experiments, as it allows for finer adjustments of stimulus contrast [48]. Participants indicated their response by a left or right arrow key press, and brief auditory feedback (50 ms tone) was provided after correct trials to maintain task engagement. As in WM task, trials started with a dynamic, centrally-presented fixation sequence. Participants completed 680 trials, split equally into 8 blocks with rest periods lasting a minimum of 30 s.

The stimulus contrast in the visual discrimination task was adjusted every trial using the Functional Adaptive Sequential Testing (FAST toolbox [78]) procedure, which determines the most informative contrast levels to be sampled for estimating participants' contrast thresholds. Two FAST structures were interleaved to estimate psychophysical functions reflecting the contrast level required to elicit reliable orientation discrimination at two different sensitivity levels (d'=1.089 and 1.634), corresponding to 70.71% and 79.37% accuracy. Of note, data analyses were completed separately from the within-task FAST procedure in order to limit biased threshold estimations from potential increased accidental error responses in SZ. See Park et al. (2017) [43] for a complete description of the psychophysical procedure.

TRANSCRANIAL DIRECT CURRENT STIMULATION

The tDCS was administered (Study 2) using a battery driven, constant current stimulator (MindAlive Inc., Alberta, Canada) and a pair of conductive rubber electrodes (active: 19.25 cm2, reference: 52 cm2). The electrodes were placed over saline-soaked sponges and each held in place with elastic cloth headbands. In the active anodal conditions, current is applied for 20 minutes. Stimulation intensity is fixed at 2.0 mA, as this intensity demonstrated improvement in visual acuity in a prior study [47]. For medial

frontal stimulation, the anodal electrode was placed over the medial frontal lobe at midline (site FCz of the International 10-20 System) and the cathodal electrode as placed over the right cheek to avoid confounding effects from other brain regions. For occipitoparietal stimulation, the anodal electrode was placed over occipitoparietal cortex at midline (site Pz of the International 10-20 System), with the cathodal electrode again placed over the right cheek. Consistent with tDCS montages in related work, the placement of the cheek electrode is on a diagonal, parallel to the jaw line, 3 cm from the lip corner (cheilion) above the jaw [47,79]. Location of anodal electrode placement over FCz or Pz was determined with individual scalp measurements. We modeled the current flow using COMETS and our previously described methods for estimating the fields generated by the stimulator [57,80].

The tDCS sham condition involves similar administration as that for the active condition, except the stimulation only lasts 30 seconds, which ramps up and down at the beginning and end of the 20-minute period. This sham procedure results in the same physical sensations (e.g., tingling, itching) that are reported with active tDCS [47]. Following each session, participants completed a questionnaire and visual analog scale that included questions regarding attention, concentration, mood, vision, headache, fatigue, and skin sensations during tDCS. Participants were additionally asked to rate whether they had received active versus sham stimulation and the degree of confidence associated with those ratings. Participants tended to overestimate the presence of stimulation, leading to an accuracy rate of detecting the correct stimulation condition of 57%. However, the hit rate for detecting sham stimulation was 15%, well below chance, suggesting that participants were blind to the sham versus active conditions. Additionally, confidence ratings did not differ across stimulus condition ($p > .23$). Scores across all questionnaire ratings did not significantly differ between stimulation conditions ($ps > .092$).

The present study followed a within-subjects design, such that each participant completed the three stimulation conditions (anodal active over medial-frontal, anodal active over occipitoparietal, and sham) on three separate days. Session order was counterbalanced across participants, and the location of sham (medial

frontal/occipitoparietal) was randomly assigned. The time interval between session visits was at least 48 hours to minimize potential task practice effects or carryover effects related to the previous session's brain stimulation (M=6.60 days between sessions, SD=4.11 days) [81].

All study sessions began with 20 minutes of active or sham tDCS applied over medial frontal or occipitoparietal cortex. Immediately after tDCS, participants completed the visual WM precision task (20-30 minutes), followed by the visual discrimination task (40-60 minutes). For the WM task, participants completed a shortened version of the visual WM task described above in order to reduce task duration and cognitive burden on participants. Participants completed a total of 60 trials, split equally into 3 blocks with rest periods lasting a minimum of 30 s. While the trial procedure was identical, memory arrays only consisted of two of four oriented gratings. In total, the two tasks lasted approximately 90 minutes, which is within the time window in which tDCS effects have been shown to last in comparable stimulation procedures [79].

ANALYSES

Visual Working Memory Task Analysis

Grating orientations were recorded and reported in the parameter space of all possible line orientation values [-90°, 90°) and converted to the circular space [-π, π) radians. Recall error on each trial was calculated as the difference between the orientation of the target grating and the orientation of the test probe that was reported (input with the manual dial) by the participant. Given that internal noise is hypothesized to add variability to, or destabilize, the internal representation [21,39], the primary performance metric of interest on the visual WM task was participants' recall variance. Poorer WM performance is thus reflected by higher recall variance, as demonstrated by the characteristic increase in recall variance (decline in precision) as the number of items remembered increases [37,38]. The Von Mises probability density function (circular normal distribution) with mean $\theta = 0$ (no error, such that recall is centered at the target memory location) and σ was used to fit every participant's distribution of recall errors at

each memory array set size. The Von Mises probability density function for a given angle x, centered at θ with a concentration κ where $I_0(\kappa)$ is the modified Bessel function of order 0:

$$f(x|\theta,\kappa) = \frac{e^{\kappa \cos(x-\theta)}}{2\pi I_0(\kappa)}.$$

The variance of the Von Mises probability density function (σ^2), which reflects the dispersion of the distribution, is analogous to the inverse of the distribution's concentration ($1/\kappa$). The concentration parameter (κ) was estimated from each participant's recall errors at every memory array set size using a maximum likelihood method. Estimates of distribution concentration were converted to variances by taking the inverse for subsequent between-group and individual differences analyses.

Orientation Discrimination Task

Data from the visual discrimination task were analyzed with two different approaches. The first involved a conventional PTM analysis to estimate model parameters at a group level, thus allowing us to test for relative groups differences in levels of noise in the three noise parameters between SZ and NT. The second approach utilized hierarchical Bayesian model fitting to estimate each individual's model parameters. The latter thus allowed for a better understanding of individual differences in noise estimates. It also enabled us to examine how noise estimates related to WM performance.

Conventional PTM Analysis. To examine group-level differences in noise estimates, visual discrimination performance was first analyzed using a conventional PTM fitting method. First, psychophysical contrast thresholds were estimated for each participant at each of the 8 external noise levels with data pooled across the two FAST structures. Individuals' contrast thresholds for orientation discrimination were estimated with Weibull functions at every external noise level using the following equation:

$$P(c) = 1 - (1 - 0.5) \times 2^{-(\frac{log\,(c)}{a})^{\eta}}$$

where P represents accuracy (percent correct), c is stimulus contrast, α is threshold at 75% accuracy, and η is the slope. The two free parameters, α and η, were estimated

with a Bayesian model fitting method implementing a Markov Chain Monte Carlo (MCMC) technique. Group averages of individuals' estimated thresholds were used to fit the conventional PTM. Coefficient indices for each noise source (unfiltered external noise (A_e), baseline internal noise (A_a), stimulus-dependent internal noise (A_m)), were introduced into the standard PTM to account for differences in noise levels between groups:

$$c_\tau = \frac{1}{\beta}\left[\frac{(1+(A_m N_m)^2)(A_e N_e)^{2\gamma} + (A_a N_a)^2}{(\frac{1}{d'^2} - (A_m N_m)^2)}\right]^{\frac{1}{2\gamma}}$$

During PTM fitting, these three SZ coefficients (A_e, A_a, A_m) could freely vary or be fixed at 1, with the latter constraining a given noise estimate to be equal across groups (Study 1) or stimulation conditions (Study 2) and the former allowing for relative differences between groups or stimulation conditions in a given noise estimate. To determine if noise sources differed between groups or conditions, all possible candidate models accounting for each combination of free and fixed noise estimates were run: the null model, which assumed no differences in any of the noise sources, the full model, which assumed differences in all three noise sources, and six remaining models reflecting the different possible combinations of the three noise estimates. In addition to which ever noise coefficients were specified to freely vary, all candidate models included the following four free parameters: stimulus-dependent internal noise (N_m), internal additive noise (N_a), signal gain from the perceptual template (β), and the exponent of the nonlinear transducer function (γ). Thus, the full model included 7 free parameters, the null model included 4 free parameters, and the other six models included between 5 and 6 free parameters. The eight candidate models were each fitted to average thresholds using a least-squares method. Candidate models were compared by evaluating differences in goodness-of-fit using r^2. The best fitting model was determined with the F-test for nested models. Specifically, the best fitting model was identified as the model with the fewest free parameters that was not significantly different from the full model, in which all parameters could freely vary.

Hierarchical Bayesian Model Analysis. A hierarchical Bayesian modeling technique was used to fit each participant's data with the PTM in order to obtain individual noise parameter estimates and examine relations between noise estimates and visual WM performance [43]. Unlike in the conventional PTM analysis approach described above, in which model parameters are estimated from the contrast thresholds at each level of external noise, the hierarchical Bayesian approach allows for model parameters to be estimated for each participant. The following PTM equation was used:

$$c_{\tau_{ij}} = \frac{1}{\beta}\left[\frac{\left(1+{N_m}^2\right)(A_f N_{e_{ij}})^{2\gamma} + {N_a}^2}{\left(\frac{1}{{d'^2}_i} - N_m^2\right)}\right]^{\frac{1}{2\gamma}}$$

where the contrast threshold is estimated at a given accuracy criterion, i (either 70.71% or 79.37%), and external noise level, j. Each participant's response on a given trial (with a given external noise level and at a given difficulty level) was assumed to be drawn from a Bernoulli distribution to capture the set of possible outcomes from the 2-alternative forced-choice response in the visual discrimination task. PTM fitting was constrained such that the gain parameter β and nonlinear power parameter γ were held constant to minimize the number of free model parameters while enabling estimation of all three noise parameters of interest (N_a, N_m, A_f) and the slope of the psychometric function (η). Values were set at β = 1 and γ = 2.64 for Study 1, and β = 1 and γ = 1.5 for Study 2, for all individuals, based on estimates generated from the conventional PTM analysis. Importantly, modifications in the values of the gain parameter β and nonlinear power parameter γ did not change the results regarding relations between noise estimates and WM recall variance. For Study 1, based on results from the conventional PTM analysis which showed a group difference in baseline internal noise and unfiltered external noise, only the N_a and A_f noise parameters were set to vary across individuals. Free model parameters were estimated for each individual with the MCMC method for sampling from posterior probability distributions. A given individual's model parameters were constrained by hierarchical priors in that parameters were assumed to be drawn from a group's (SZ or NT) population distribution with their own means and SDs. Priors for the two groups were set to broad uniform distributions.

Statistics

Repeated measures ANOVAs were conducted to determine changes in recall variance with increasing WM set size and to probe group differences (Study1) and effects of tDCS locations (Study 2). To assess the relationship between the sensory noise estimates and WM variance, multiple linear regressions were completed within each group. Nested F-tests were used to compare different models of PTM with varying numbers of free parameters. Statistical analyses were performed at the significance level of .05.

DATA AVAILABILITY

The data generated and/or analyzed during the current study are not publicly available due to participant confidentiality concerns. Although the data do not contain direct identifiers, they include information that, in combination (e.g., location, patient group), may pose a risk of re-identification. De-identified data will be made available from the corresponding authors on request, subject to institutional review and approval.

CODE AVAILABILITY

Code to run experiments and analyze data (MATLAB and Python) are available on Github repository: https://github.com/gt-core-lab/wm-noise-sz.

ACKNOWLEDGMENTS

Supported by the NIH (R00-EY034546 to WJP; T32-EY007135, P30-EY08126 to GFW; R01-MH110378 to GFW and SP, R01-MH073028, R01-MH128967 to SP), Smithgall Watts Early Career Award to WJP, Brain & Behavior Research Foundation (NARSAD Independent Investigator Grant to DT; Distinguished Investigator Grant to SP), NSF (BCS-2147064 to GFW), the E. Bronson Ingram Family (to GFW), American

Psychological Foundation (Alexander Gralnick Research Investigator Award to SP), and Gertrude Conaway Vanderbilt Endowment (to SP).

AUTHOR CONTRIBUTIONS

Conceptualization: WJP, MI, GFW, DT, and SP; Methodology: WJP, MI, GFW, DT, and SP; Software: WJP, and MI; Formal analysis: WJP, GH, and MI; Investigation: WJP, and MI.; Writing—Original draft: MI; Writing—Review & Editing: WJP, MI, GFW, DT, and SP; Funding acquisition: GFW, DT, and SP.

COMPETING INTERESTS

The authors declare no competing interests.

REFERENCES

1. Postle, B. R. Cognitive neuroscience of visual working memory. in *Working memory: State of the science* 333–357 (2021).
2. Brady, T. F., Konkle, T. & Alvarez, G. A. A review of visual memory capacity: Beyond individual items and toward structured representations. *Journal of Vision* **11**, 4–4 (2011).
3. Luck, S. J. Visual short-term memory. in *Visual memory* (2008).
4. Ma, W. J., Husain, M. & Bays, P. M. Changing concepts of working memory. *Nature Neuroscience* **17**, 347–356 (2014).
5. Barnes-Scheufler, C. V. *et al.* Transdiagnostic comparison of visual working memory capacity in bipolar disorder and schizophrenia. *Int J Bipolar Disord* **9**, 12 (2021).

6. Kensinger, E. A., Shearer, D. K., Locascio, J. J., Growdon, J. H. & Corkin, S. Working memory in mild Alzheimer's disease and early Parkinson's disease. *Neuropsychology* **17**, 230–239 (2003).
7. Moran, T. P. Anxiety and Working Memory Capacity: A Meta-Analysis and Narrative Review. (2016).
8. Park, S. & Gooding, D. C. Working memory impairment as an endophenotypic marker of a schizophrenia diathesis. *Schizophrenia Research: Cognition* **1**, 127–136 (2014).
9. Park, S. & Holzman, P. S. Schizophrenics show spatial working memory deficits. *Archives of General Psychiatry* **49**, 975–982 (1992).
10. Xie, W., Campbell, S. & Zhang, W. Working memory capacity predicts individual differences in social-distancing compliance during the COVID-19 pandemic in the United States. *Proc. Natl. Acad. Sci. U.S.A.* **117**, 17667–17674 (2020).
11. Eriksson, J., Vogel, E. K., Lansner, A., Bergström, F. & Nyberg, L. Neurocognitive Architecture of Working Memory. *Neuron* **88**, 33–46 (2015).
12. Hakim, N., Adam, K. C. S., Gunseli, E., Awh, E. & Vogel, E. K. Dissecting the Neural Focus of Attention Reveals Distinct Processes for Spatial Attention and Object-Based Storage in Visual Working Memory. *Psychological Science* **30**, 526–540 (2019).
13. Lin, H.-Y. & Oberauer, K. An interference model for visual working memory: Applications to the change detection task. *Cognitive Psychology* **133**, 101463 (2022).

14. Buschman, T. J., Siegel, M., Roy, J. E. & Miller, E. K. Neural substrates of cognitive capacity limitations. *Proc. Natl. Acad. Sci. U.S.A.* **108**, 11252–11255 (2011).
15. Gazzaley, A. & Nobre, A. C. Top-down modulation: bridging selective attention and working memory. *Trends in Cognitive Sciences* **16**, 129–135 (2012).
16. Goldman-Rakic, P. S. & Selemon, L. D. Functional and Anatomical Aspects of Prefrontal Pathology in Schizophrenia. *Schizophrenia Bulletin* **23**, 437–458 (1997).
17. Scimeca, J. M., Kiyonaga, A. & D'Esposito, M. Reaffirming the Sensory Recruitment Account of Working Memory. *Trends in Cognitive Sciences* **22**, 190–192 (2018).
18. Xu, Y. Reevaluating the Sensory Account of Visual Working Memory Storage. *Trends in Cognitive Sciences* **21**, 794–815 (2017).
19. Zhao, Y.-J., Kay, K. N., Tian, Y. & Ku, Y. Sensory Recruitment Revisited: Ipsilateral V1 Involved in Visual Working Memory. *Cerebral Cortex* **32**, 1470–1479 (2022).
20. Luck, S. J. & Vogel, E. K. Visual working memory capacity: From psychophysics and neurobiology to individual differences. *Trends in Cognitive Sciences* **17**, 391–400 (2013).
21. Bays, P. M. Noise in Neural Populations Accounts for Errors in Working Memory. *Journal of Neuroscience* **34**, 3632–3645 (2014).
22. Dosher, B. A. & Lu, Z. L. Perceptual learning reflects external noise filtering and internal noise reduction through channel reweighting. *Proceedings of the National Academy of Sciences* **95**, 13988–13993 (1998).
23. Faisal, A. A., Selen, L. P. J. & Wolpert, D. Noise in the nervous system. *Nature Reviews Neuroscience* **9**, 292–303 (2008).

24. Shannon, C. E. A Mathematical Theory of Communication. *Bell System Technical Journal* **27**, 379–423 (1948).
25. Harrison, S. A. & Tong, F. Decoding reveals the contents of visual working memory in early visual areas. *Nature* **458**, 632–635 (2009).
26. Pasternak, T. & Greenlee, M. W. Working memory in primate sensory systems. *Nature Reviews Neuroscience* **6**, 97–107 (2005).
27. Vogel, E. K. & Machizawa, M. G. Neural activity predicts individual differences in visual working memory capacity. *Nature* **428**, 748–751 (2004).
28. Castner, StacyA., Goldman-Rakic, PatriciaS. & Williams, GrahamV. Animal models of working memory: insights for targeting cognitive dysfunction in schizophrenia. *Psychopharmacology* **174**, (2004).
29. Barch, D. M. & Ceaser, A. Cognition in schizophrenia: core psychological and neural mechanisms. *Trends in Cognitive Sciences* **16**, 27–34 (2012).
30. Javitt, D. C. When Doors of Perception Close: Bottom-up Models of Disrupted Cognition in Schizophrenia. *Annu. Rev. Clin. Psychol.* **5**, 249–275 (2009).
31. Kim, J., Park, S. & Blake, R. Perception of biological motion in Schizophrenia and healthy individuals: A behavioral and fMRI study. *PLoS ONE* **6**, (2011).
32. Tadin, D. *et al.* Weakened center-surround interactions in visual motion processing in schizophrenia. *Journal of Neuroscience* **26**, 11403–11412 (2006).
33. Yang, E. *et al.* Visual context processing in schizophrenia. *Clinical psychological science* **1**, 5–15 (2013).

34. Abbasi, S., Wolff, A., Çatal, Y. & Northoff, G. Increased noise relates to abnormal excitation-inhibition balance in schizophrenia: a combined empirical and computational study. *Cerebral Cortex* **33**, 10477–10491 (2023).
35. Chen, Y., Norton, D. & McBain, R. Effects of domain-specific noise on visual motion processing in schizophrenia. *PLoS ONE* **9**, (2014).
36. Christensen, B. K., Spencer, J. M. Y., King, J. P., Sekuler, A. B. & Bennett, P. J. Noise as a mechanism of anomalous face processing among persons with Schizophrenia. *Front. Psychol.* **4**, (2013).
37. Bays, P. M. & Husain, M. Dynamic Shifts of Limited Working Memory Resources in Human Vision. *Science* **321**, 851–854 (2008).
38. Wilken, P. & Ma, W. J. A detection theory account of change detection. *Journal of vision* **4**, 1120–35 (2004).
39. Starc, M. *et al.* Schizophrenia is associated with a pattern of spatial working memory deficits consistent with cortical disinhibition. *Schizophrenia Research* **181**, 107–116 (2017).
40. Pelli, D. G. & Farell, B. Why use noise? *Journal of the Optical Society of America. A, Optics, image science, and vision* **16**, 647–653 (1999).
41. Dosher, B. A. & Lu, Z. Noise exclusion in spatial attention. *Psychological Science* **11**, 139–146 (2000).
42. Manning, C., Dakin, S. C., Tibber, M. S. & Pellicano, E. Averaging, not internal noise, limits the development of coherent motion processing. *Developmental cognitive neuroscience* **10**, 1–13 (2014).

43. Park, W. J., Schauder, K. B., Zhang, R., Bennetto, L. & Tadin, D. High internal noise and poor external noise filtering characterize perception in autism spectrum disorder. *Scientific Reports* 1–12 (2017).

44. Nitsche, M. A. & Paulus, W. Excitability changes induced in the human motor cortex by weak transcranial direct current stimulation. *The Journal of Physiology* **527**, 633–639 (2000).

45. Nitsche, M. A. & Paulus, W. Sustained excitability elevations induced by transcranial DC motor cortex stimulation in humans. *Neurology* **57**, 1899–1901 (2001).

46. Wagner, T., Valero-Cabre, A. & Pascual-Leone, A. Noninvasive Human Brain Stimulation. *Annu. Rev. Biomed. Eng.* **9**, 527–565 (2007).

47. Reinhart, R. M. G., Xiao, W., McClenahan, L. J. & Woodman, G. F. Electrical Stimulation of Visual Cortex Can Immediately Improve Spatial Vision. *Current Biology* **26**, 1867–1872 (2016).

48. Lu, Z.-L. & Dosher, B. A. Perceptual learning retunes the perceptual template in foveal orientation identification. *Journal of vision* **4**, 44–56 (2004).

49. Mayer, J. S. & Park, S. Working memory encoding and false memory in schizophrenia and bipolar disorder in a spatial delayed response task. *Journal of Abnormal Psychology* **121**, 784–794 (2012).

50. Thakkar, K. N. & Park, S. Impaired Passive Maintenance and Spared Manipulation of Internal Representations in Patients With Schizophrenia. *Schizophrenia Bulletin* **38**, 787–795 (2012).

51. D'Esposito, M. From cognitive to neural models of working memory. *Phil. Trans. R. Soc. B* **362**, 761–772 (2007).

52. Tsubomi, H., Fukuda, K., Watanabe, K. & Vogel, E. K. Neural Limits to Representing Objects Still within View. *J. Neurosci.* **33**, 8257–8263 (2013).

53. Adam, K. C. S., Mance, I., Fukuda, K. & Vogel, E. K. The Contribution of Attentional Lapses to Individual Differences in Visual Working Memory Capacity. *Journal of Cognitive Neuroscience* **27**, 1601–1616 (2015).

54. Wang, J.-K. *et al.* Enhancing visual working memory in schizophrenia: effects of frontoparietal theta tACS in low-performing patients. *Schizophr* **10**, 97 (2024).

55. Rokem, A. *et al.* Broader Visual Orientation Tuning in Patients with Schizophrenia. *Frontiers in Human Neuroscience* **5**, 127 (2011).

56. Boroda, E., Sponheim, S. R., Fiecas, M. & Lim, K. O. Transcranial direct current stimulation (tDCS) elicits stimulus-specific enhancement of cortical plasticity. *NeuroImage* **211**, 116598 (2020).

57. Reinhart, R. M. G., Cosman, J. D., Fukuda, K. & Woodman, G. F. Using transcranial direct-current stimulation (tDCS) to understand cognitive processing. *Atten Percept Psychophys* **79**, 3–23 (2017).

58. Antal, A., Kincses, T. Z., Nitsche, M. A., Bartfai, O. & Paulus, W. Excitability Changes Induced in the Human Primary Visual Cortex by Transcranial Direct Current Stimulation: Direct Electrophysiological Evidence. *Invest. Ophthalmol. Vis. Sci.* **45**, 702 (2004).

59. Uhlhaas, P. J., Phillips, W. A. & Silverstein, S. M. The course and clinical correlates of dysfunctions in visual perceptual organization in schizophrenia during the remission of psychotic symptoms. *Schizophrenia Research* **75**, 183–192 (2005).

60. Dinstein, I. *et al.* Unreliable evoked responses in autism. *Neuron* **75**, 981–991 (2012).
61. Habib, A., Harris, L., Pollick, F. & Melville, C. A meta-analysis of working memory in individuals with autism spectrum disorders. *PLoS ONE* **14**, e0216198 (2019).
62. Wang, Y. *et al.* A Meta-Analysis of Working Memory Impairments in Autism Spectrum Disorders. *Neuropsychol Rev* **27**, 46–61 (2017).
63. Calvin, O. L. & Redish, A. D. Global disruption in excitation-inhibition balance can cause localized network dysfunction and Schizophrenia-like context-integration deficits. *PLoS Comput Biol* **17**, e1008985 (2021).
64. Gao, R. & Penzes, P. Common Mechanisms of Excitatory and Inhibitory Imbalance in Schizophrenia and Autism Spectrum Disorders. *CMM* **15**, 146–167 (2015).
65. Rubenstein, J. L. R. & Merzenich, M. M. Model of autism: Increased ratio of excitation/inhibition in key neural systems. *Genes, brain, and behavior* **2**, 255–267 (2003).
66. Fried, R. *et al.* Clinical correlates of working memory deficits in youth with and without ADHD: A controlled study. *Journal of Clinical and Experimental Neuropsychology* **38**, 487–496 (2016).
67. Jeffries, S. & Everatt, J. Working memory: Its role in dyslexia and other specific learning difficulties. *Dyslexia* **10**, 196–214 (2004).
68. Kessels, R. P. C., Molleman, P. W. & Oosterman, J. M. Assessment of working-memory deficits in patients with mild cognitive impairment and Alzheimer's dementia using Wechsler's Working Memory Index. *Aging Clin Exp Res* **23**, 487–490 (2011).

69. Lee, J. & Park, S. Working Memory Impairments in Schizophrenia: A Meta-Analysis. *Journal of Abnormal Psychology* **114**, 599–611 (2005).

70. First, M. B., Spitzer, R. L., Gibbon, M. & Williams, J. B. W. First, M. B., Spitzer, R. L., Gibbon, M., & Williams, J. B. W. (2002). Structured clinical interview for DSM-IV-TR axis I disorders, research version, patient edition. (SCID-I/P). *Biometrics Research* (2002).

71. Nelson, H. E. National Adult Reading Test (NART): For the Assessment of Premorbid Intelligence in Patients with Dementia: Test Manual. (1982).

72. Andreasen, N. C. Scale for the assessment of negative symptoms (SANS). *Iowa City: University of Iowa.* (1983).

73. Andreasen, N. C. Scale for the assessment of positive symptoms (SAPS). *University of Iowa: Iowa City.* (1984).

74. Brainard, D. H. The Psychophysics Toolbox. *Spatial Vision* **10**, 433–436 (1997).

75. Pelli, D. G. The VideoToolbox software for visual psychophysics: Transforming numbers into movies. *Spatial Vision* **10**, 437–442 (1997).

76. Foss-Feig, J., Tadin, D., Schauder, K. B. & Cascio, C. J. A substantial and unexpected enhancement of motion perception in autism. *Journal of Neuroscience* **33**, 8243–8249 (2013).

77. Gold, J. M. *et al.* Reduced Capacity but Spared Precision and Maintenance of Working Memory Representations in Schizophrenia. *Arch Gen Psychiatry* **67**, 570 (2010).

78. Vul, E., Bergsma, J. & MacLeod, D. I. Functional Adaptive Sequential Testing. *Seeing and Perceiving* **23**, 483–515 (2010).

79. Reinhart, R. M. G. & Woodman, G. F. Causal Control of Medial–Frontal Cortex Governs Electrophysiological and Behavioral Indices of Performance Monitoring and Learning. *J. Neurosci.* **34**, 4214–4227 (2014).

80. Jung, Y.-J., Kim, J.-H. & Im, C.-H. COMETS: A MATLAB toolbox for simulating local electric fields generated by transcranial direct current stimulation (tDCS). *Biomed. Eng. Lett.* **3**, 39–46 (2013).

81. Monte-Silva, K. *et al.* Induction of Late LTP-Like Plasticity in the Human Motor Cortex by Repeated Non-Invasive Brain Stimulation. *Brain Stimulation* **6**, 424–432 (2013).